Pivotal role of the transcriptional co-activator YAP in trophoblast stemness of the developing human placenta

Gudrun Meinhardt[a], Sandra Haider[a], Victoria Kunihs[a], Leila Saleh[a], Jürgen Pollheimer[a], Christian Fiala[b], Szabolcs Hetey[c], Zsofia Feher[c], Andras Szilagyi[c], Nandor Gabor Than[c,d,e], and Martin Knöfler[a,1]

[a]Department of Obstetrics and Gynaecology, Reproductive Biology Unit, Medical University of Vienna, A-1090 Vienna, Austria; [b]Gynmed Clinic, A-1150 Vienna, Austria; [c]Systems Biology of Reproduction Lendulet Group, Institute of Enzymology, Research Centre for Natural Sciences, H-1117 Budapest, Hungary; [d]Maternity Private Clinic of Obstetrics and Gynecology, H-1126 Budapest, Hungary; and [e]1st Department of Pathology and Experimental Cancer Research, Semmelweis University, H-1085 Budapest, Hungary

Edited by R. Michael Roberts, University of Missouri, Columbia, MO, and approved April 30, 2020 (received for review February 12, 2020)

Various pregnancy complications, such as severe forms of preeclampsia or intrauterine growth restriction, are thought to arise from failures in the differentiation of human placental trophoblasts. Progenitors of the latter either develop into invasive extravillous trophoblasts, remodeling the uterine vasculature, or fuse into multinuclear syncytiotrophoblasts transporting oxygen and nutrients to the growing fetus. However, key regulatory factors controlling trophoblast self-renewal and differentiation have been poorly elucidated. Using primary cells, three-dimensional organoids, and CRISPR-Cas9 genome-edited JEG-3 clones, we herein show that YAP, the transcriptional coactivator of the Hippo signaling pathway, promotes maintenance of cytotrophoblast progenitors by different genomic mechanisms. Genetic or chemical manipulation of YAP in these cellular models revealed that it stimulates proliferation and expression of cell cycle regulators and stemness-associated genes, but inhibits cell fusion and production of syncytiotrophoblast (STB)-specific proteins, such as hCG and GDF15. Genome-wide comparisons of primary villous cytotrophoblasts overexpressing constitutively active YAP-5SA with YAP KO cells and syncytializing trophoblasts revealed common target genes involved in trophoblast stemness and differentiation. ChIP-qPCR unraveled that YAP-5SA overexpression increased binding of YAP–TEAD4 complexes to promoters of proliferation-associated genes such as *CCNA* and *CDK6*. Moreover, repressive YAP–TEAD4 complexes containing the histone methyltransferase EZH2 were detected in the genomic regions of the STB-specific *CGB5* and *CGB7* genes. In summary, YAP plays a pivotal role in the maintenance of the human placental trophoblast epithelium. Besides activating stemness factors, it also directly represses genes promoting trophoblast cell fusion.

placenta | trophoblast | stemness

The human placenta represents a unique exchange organ between the expectant mother and the developing fetus. It fulfills a plethora of biological functions required for a successful pregnancy, including immunological tolerance of the semiallogenic conceptus, adaption of the mother's endocrine system, remodeling of the maternal uterine vasculature, and, most importantly, fetal nutrition (1–4). Rapid development of the placenta and its two differentiated epithelial trophoblast subtypes, multinucleated syncytiotrophoblasts (STBs) and invasive extravillous trophoblasts (EVTs), within the first weeks of gestation is a prerequisite for the maintenance of pregnancy. Whereas EVTs migrate into the maternal uterus and remodel its vessels, STBs secrete pregnancy hormones into the maternal circulation and deliver nutrients and oxygen to the growing fetus. Failures in placentation were noticed in a variety of pregnancy complications, such as early-onset preeclampsia, severe intrauterine growth restriction (IUGR), miscarriage, preterm labor, and stillbirth (5–8). In these disorders, impaired remodeling of the maternal spiral arteries, a process adjusting blood flow to the developing placenta, might cause malperfusion and, as a consequence, oxidative-stress provoking placental dysfunction (9–11). Besides fetal and maternal aberrations, failures in placentation are thought to arise from abnormal trophoblast differentiation (12). Indeed, cytotrophoblasts (CTBs) isolated from preeclamptic placentae exhibit defects in in vitro EVT formation (13). Likewise, CTB growth and/or cell fusion were shown to be impaired in cultures established from placental tissues of pregnancies with preeclampsia, IUGR, or trisomy 21 (14–18). However, the molecular mechanisms underlying gestational disease are largely unknown. Equally, key regulatory factors controlling stemness and trophoblast subtype formation and differentiation in the developing human placenta remain poorly defined.

One such pathway potentially regulating trophoblast lineage formation and placental expansion could be the Hippo signaling cascade. Previous investigations suggested that this particular pathway plays an important role during development by controlling organ size, tissue regeneration, cell fate decisions,

Significance

Defects in development and differentiation of the placenta are associated with various pregnancy disorders such as miscarriage, stillbirth, preeclampsia, and intrauterine growth restriction. However, our knowledge on critical regulators of human placentation is scarce. In the present study, we show that the Hippo signaling-dependent transcriptional coactivator YAP plays a pivotal role in the maintenance of proliferative trophoblasts, the epithelial cells of the placenta. By binding to the transcription factor TEAD4, YAP stimulates expression of genes promoting trophoblast stemness. Additionally, YAP–TEAD4 complexes actively repress genes associated with the differentiated syncytiotrophoblast, the hormone-secreting cell type of the human placenta. Hence, YAP orchestrates a complex developmental program ensuring growth and expansion of the human placenta.

Author contributions: G.M., S. Haider, V.K., L.S., and J.P. performed research; C.F. contributed new reagents/analytic tools; S. Hetey, Z.F., A.S., and N.G.T. analyzed data; and M.K. wrote the paper.

The authors declare no competing interest.

This article is a PNAS Direct Submission.

Data deposition: Raw RNA-seq data are accessible at the Gene Expression Omnibus (GEO) database (https://www.ncbi.nlm.nih.gov/geo/) under accession nos. GSE143858, GSE143859, and GSE143860.

[1]To whom correspondence may be addressed. Email: martin.knoefler@meduniwien.ac.at.

This article contains supporting information online at https://www.pnas.org/lookup/suppl/doi:10.1073/pnas.2002630117/-/DCSupplemental.

First published June 1, 2020.

stemness, and differentiation (19–22). Activation of canonical Hippo signaling occurs through numerous triggers, such as biomechanical cues, high cell density, cell polarity, and G protein-coupled receptor signaling, provoking sequential phosphorylation of MST1/2 protein kinases and their downstream targets, the large tumor suppressor kinases 1/2 (LATS1/2) (23). Active LATS1/2 then phosphorylates the key components of Hippo signaling, Yes-associated protein (YAP) and transcriptional coactivator with PDZ-binding motif (TAZ), also known as WW domain containing transcription regulator 1 (WWTR1), resulting in their inactivation by either proteasomal degradation or cytoplasmic retention upon binding to 14–3-3 (19). However, in the Hippo-off state, unphosphorylated YAP/TAZ are recruited to the nucleus, where they promote stemness and proliferation by acting as coactivators of the TEA domain (TEAD) transcription factor family (24). YAP–TEAD4 transcriptional complexes then cooperate with different other transcription factors, for example, AP1, MYC, or E2F, to promote cell cycle progression of primary and tumor cells (25). Notably, YAP–TEAD4 was also shown to be critical for murine trophectoderm (TE) development by activating Cdx2 and other key regulators of TE in outer cells of preimplantation embryos (26). TEAD4 also localizes to trophoblasts of mouse (27) and human placenta. In the latter, TEAD4 mainly localizes to the nuclei of proliferative villous CTBs (vCTBs), suggesting that it could be necessary for trophoblast maintenance and expansion (27, 28). Indeed, TEAD4 has also been detected in nuclei of human trophoblast stem cells (TSCs) and self-renewing CTBs of three-dimensional (3D) trophoblast organoid cultures (TB-ORGs) (29, 30). However, functional analyses of TEAD4 and other TEAD proteins in human trophoblasts are lacking. Moreover, detailed expression patterns of the TEAD coactivators YAP/TAZ, their interaction partners, and specific tasks in human trophoblasts have not been unraveled. Using primary vCTBs, JEG-3 YAP knock-out (KO) clones, and 3D TB-ORGs, we herein demonstrate that YAP plays a pivotal role in trophoblast proliferation and expansion. Besides activating cell cycle and stemness genes, YAP–TEAD4 complexes also directly suppress genes promoting trophoblast cell fusion.

Results

Nuclear YAP Expression Is Associated with Self-Renewing Cytotrophoblasts. Tissue and cellular distribution of YAP was analyzed in first-trimester placental samples, primary trophoblast subtypes, and long-term expanding TB-ORGs (Fig. 1). Immunofluorescence, Western blotting, and quantitative PCR (qPCR) revealed that YAP was present in nuclei and cytoplasm of vCTBs, whereas EVTs only weakly expressed the particular gene (Fig. 1 *A*–*C*). YAP was absent from STB, and its protein expression decreased during in vitro cell fusion of first-trimester primary vCTBs, while glial cells missing-1 (GCM1), the regulator of fusogenic syncytins (31), and human chorionic gonadotrophin β (CGβ) increased (Fig. 1*A* and *SI Appendix*, Fig. S1 *A* and *B*). In the proximal cell column, YAP predominantly localized to the membrane and cytoplasm, whereas actively dividing, E-cadherin$^+$ CTBs of TB-ORGs mainly showed nuclear expression (Fig. 1*A*). In contrast, TAZ was predominantly detected in nuclei of EVTs, but only weakly expressed in vCTBs and proximal cell column trophoblasts (CCTs; Fig. 1 *A*–*C* and *SI Appendix*, Fig. S1*C*). The YAP/TAZ-binding TEAD proteins were also differentially expressed between trophoblast subtypes. Whereas TEAD1 protein and mRNA were primarily observed in EVTs, TEAD4 was mainly present in vCTBs, and decreased during EVT formation (*SI Appendix*, Fig. S1 *D* and *E*), as previously shown (27, 28). TEAD2 was largely associated with EVTs, while TEAD3 was ubiquitously expressed among the different trophoblast subtypes (*SI Appendix*, Fig. S1 *D* and *E*). Coimmunoprecipitation and Western blotting revealed that YAP predominantly interacts with TEAD4 in first-trimester vCTBs (*SI Appendix*, Fig. S1*F*).

YAP Up-Regulates Stemness and Cell Cycle Genes but Suppresses Regulators and Markers of Trophoblast Cell Fusion. YAP was genetically manipulated in primary vCTBs and trophoblastic JEG-3 cells using overexpression and CRISPR-Cas9–mediated genome editing, respectively (Fig. 2). Constitutive active YAP-5SA harbors five serine-to-alanine mutations (Fig. 2*A*) abolishing LATS phosphorylation and binding to 14–3-3 (32). Overexpression of YAP-5SA diminished TAZ protein levels (Fig. 2*B*), as reported (33), and increased luciferase activity of a synthetic TEAD reporter, whereas a mutant lacking the C-terminal PDZ binding motif for nuclear retention (YAP-ΔC) (34) was less active (*SI Appendix*, Fig. S2*A*). In contrast to that, TAZ was up-regulated in the four YAP KO clones established by genome editing (Fig. 2*C* and *SI Appendix*, Fig. S2*B*). Subsequently, RNA-seq of YAP-5SA–overexpressing vCTB cultures, YAP KO clones, and untransfected vCTB cells undergoing cell fusion (20 and 72 h of cultivation) was performed (35–37). Bioinformatic analyses revealed that 513 mRNAs were up-regulated by YAP-5SA, including stemness-, cell cycle-, and mitosis-associated genes controlled by TEAD–YAP complexes (25), whereas 500 mRNAs, including STB-specific transcripts, were suppressed by the constitutively active YAP mutant (Dataset S1 and *SI Appendix*, Fig. S2*C*). Accordingly, numerous regulators of proliferation were detected among the 632 genes down-regulated in the YAP KO clones, while hormones and other markers of STB were elevated (Dataset S2 and *SI Appendix*, Fig. S2*D*). Comparisons of mRNAs differentially expressed during cell fusion (Dataset S3 and *SI Appendix*, Fig. S2*E*) with YAP-5SA–overexpressing vCTBs and the YAP KO clones delineated common YAP targets in the three cell populations (Fig. 2*D* and Dataset S4). Subsequent qPCR and Western blot analyses of selected target genes in differentiating vCTBs (Fig. 3) revealed that YAP-5SA increased expression of stemness/proliferation-associated genes such as cyclin A (CCNA), cyclin-dependent kinase 6 (CDK6), cysteine-rich angiogenic inducer 61 (CYR61), TEAD4, page family member 4 (*PAGE4*), and integrin α6 (*ITGA6*; Fig. 3 *A* and *B* and *SI Appendix*, Fig. S3*A*), but down-regulated STB markers, i.e., CGβ, *GCM1*, ovo-like transcriptional repressor 1 (*OVOL1*), poly(U)-specific endoribonuclease (ENDOU), and growth differentiation factor 15 (GDF15; Fig. 3 *C*–*E* and *SI Appendix*, Fig. S3*A*). In agreement with that, YAP KO and/or combined YAP/TAZ gene silencing in JEG-3 cells or vCTBs decreased CYR61, CDK6, *TP63*, and TEAD4, while CGβ and ENDOU were elevated (*SI Appendix*, Fig. S3 *B*–*F*). Despite its low expression in first-trimester vCTB preparations (38), *CDX2* was also significantly up-regulated in YAP-5SA–overexpressing vCTB cultures (*SI Appendix*, Fig. S3*A*).

YAP Promotes Trophoblast Expansion and Inhibits Cell Fusion. The biological role of YAP was evaluated in primary vCTBs and YAP KO cells, both cultivated in 2D as well as in 3D (Fig. 4). In agreement with its positive effects on cell cycle genes, YAP-5SA overexpression increased EdU labeling in 2D-cultivated vCTBs and decreased apoptosis (Fig. 4*A* and *SI Appendix*, Fig. S4*A*). However, YAP KO or siRNA-mediated gene silencing did not alter 2D proliferation of JEG-3 cells, suggesting compensatory effects of up-regulated TAZ in these cells (Fig. 4*B* and *SI Appendix*, Fig. S4*B*). Cell numbers of YAP KO cells were only affected when TAZ was additionally down-regulated with siRNAs. The latter condition also elevated expression of the keratin 18 neoepitope (*SI Appendix*, Fig. S4*C*). Further, YAP-5SA suppressed 2D cell fusion of primary vCTBs, while silencing of YAP/TAZ increased it (Fig. 4*C* and *SI Appendix*, Fig. S4*D*). Accordingly, YAP KO alone or in combination with TAZ gene silencing also enhanced 2D STB formation in JEG-3 cells (Fig. 4*D*).

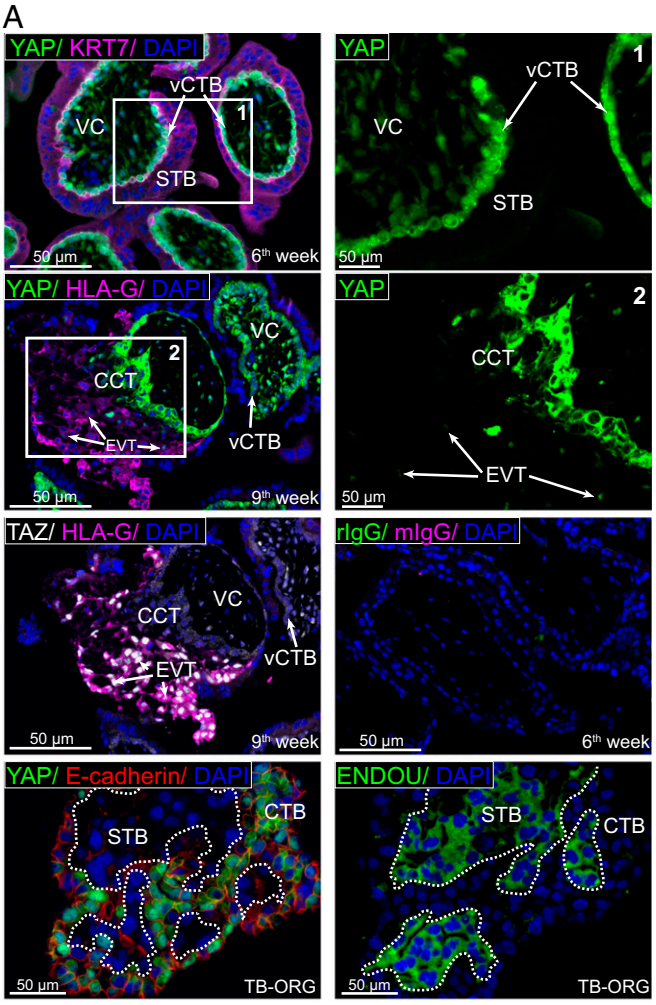

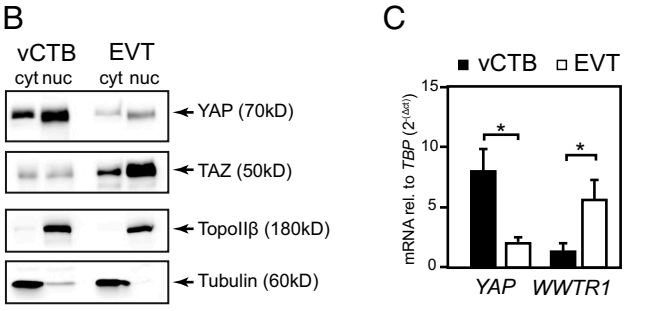

Fig. 1. Expression and localization of the transcriptional coactivators YAP/TAZ in first-trimester placenta, purified trophoblast subtypes, and 3D organoids. (*A*) Immunofluorescence in first-trimester placenta and trophoblast organoids (TB-ORGs). Representative images of placentae from sixth to ninth week of gestation ($n = 7$) and of a TB-ORG ($n = 4$ cultures, derived from single sixth- to seventh-week placentae and analyzed between passage 2 and 4) are shown. Higher magnifications of inset pictures (*1*, *2*) with single YAP staining are shown on the right side. Cytokeratin 7 (KRT7) and HLA-G were used as markers of trophoblast and EVT, respectively. In negative controls, primary antibodies were replaced by rabbit IgG (rIgG) and/or mouse IgG (mIgG). DAPI marks nuclei. CCT, cell column trophoblast; EVT, extravillous trophoblast; STB, syncytiotrophoblasts, VC, villous core; vCTB, villous cytotrophoblast. Poly(U)-specific endoribonuclease (ENDOU), previously identified as STB marker (29), was used to delineate fused areas (bordered by stippled lines) in TB-ORGs. (*B*) Representative Western blot showing intracellular distribution of YAP/TAZ in purified first-trimester trophoblast subtypes ($n = 3$ different vCTB and EVT preparations, each isolated from three or four pooled sixth- to ninth-week placentae). Topoisomerase IIβ (TopoIIβ) and tubulin were used to visualize purity of nuclear (nuc) and cytoplasmic (cyt) extracts. (*C*) Expression of *YAP* and *WWTR1* mRNAs, encoding TAZ, in purified vCTB ($n = 3$) and EVT ($n = 3$) cell pools, measured by RT-qPCR. Data were normalized to transcript levels of TATA box binding protein (*TBP*). Mean values ± SEM are depicted (*$P < 0.05$).

Treatment of self-renewing 3D TB-ORGs, prepared from primary vCTBs, with low doses of the chemical YAP/TAZ inhibitor verteporfin inhibited organoid growth and cyclin A expression, resulting in the loss of the outer proliferative CTB layer, whereas survival was not affected (Fig. 4*E* and *SI Appendix*, Fig. S4*E*). Similarly, organoids established from the JEG-3 YAP KO clones (*SI Appendix*, Fig. S4*F*) expressed less TEAD4 and up-regulated CGβ and ENDOU, suggesting premature differentiation (Fig. 4 *F* and *G* and *SI Appendix*, Fig. S4*G*).

YAP–TEAD4 Complexes Interact with Genomic Regions of Both Cell Cycle Regulators and Syncytiotrophoblast-Specific Genes. To assess a direct involvement of YAP–TEAD4 complexes in the up-regulation of cell cycle genes, genomic sequences of *CCNA2* and *CDK6*, previously shown to bind YAP and TEAD4 (39, 40), were analyzed by chromatin immunoprecipitation (ChIP)-qPCR using YAP and TEAD4 antibodies. In accordance with elevated transcript levels, binding of YAP to the enhancer and promoter region of *CCNA2* and *CDK6*, respectively, was reinforced in YAP-5SA–overexpressing vCTBs, whereas binding of the methyltransferase enhancer of zeste 2 (EZH2), provoking trimethylation of histone H3 lysine 27 (H3K27me3), was diminished (*SI Appendix*, Fig. S5*A*). Both YAP and TEAD4 also directly bound to promoter sequences of the STB-specific genes *CGB5* and *CGB7* (Fig. 5). Previously identified TEAD4 binding sites in these genes were retrieved from the GTRD databases (Fig. 5*A*). Primers spanning these sites were utilized for qPCR after ChIP (*SI Appendix*, Table S2). Notably, interaction of EZH2 with the genomic regions of *CGB5* and *CGB7* and the gene-repressive histone mark H3K27me3 were increased in the presence of constitutively active YAP (Fig. 5*B*). In contrast, two predicted TEAD4 binding regions of the *OVOL1* gene were not affected (*SI Appendix*, Fig. S5*B*). In summary, YAP could maintain trophoblast stemness by activating proliferation, but also by directly repressing STB-specific genes and regulators of cell fusion.

Discussion

Rapid growth and formation of differentiated trophoblast subtypes during the first weeks of gestation are critical for a successful pregnancy, since failures in these processes have been noticed in various pregnancy disorders. However, key regulatory factors and pathways controlling human placental development have been poorly defined (38). Yet, the derivation of long-term expanding TSCs and organoids gave novel insights into signaling cascades required for TSC/progenitor cell expansion and differentiation (29, 30, 42). In these studies, epidermal growth factor (EGF) signaling, inhibition of transforming growth factor-β (TGF-β) signaling, and activation of the canonical Wingless (Wnt) pathway were delineated as critical factors of trophoblast self-renewal, whereas loss of Wnt and induction of Notch1-mediated signaling promoted formation of progenitors of the EVT lineage (28, 29). Hence, a complex network of signaling cascades and mediators is thought to control TSC expansion, progenitor formation, and differentiation. Notably, canonical Wnt signaling has been implicated in both trophoblast self-renewal and EVT differentiation, operating through different downstream effectors of the T cell factor (TCF) family (29, 43, 44). Therefore, the specific roles of key regulators strongly depend on the cellular context in the developing human placenta.

The latter also seems to apply to the functions of the Hippo signaling-dependent coactivators YAP and TAZ in the early

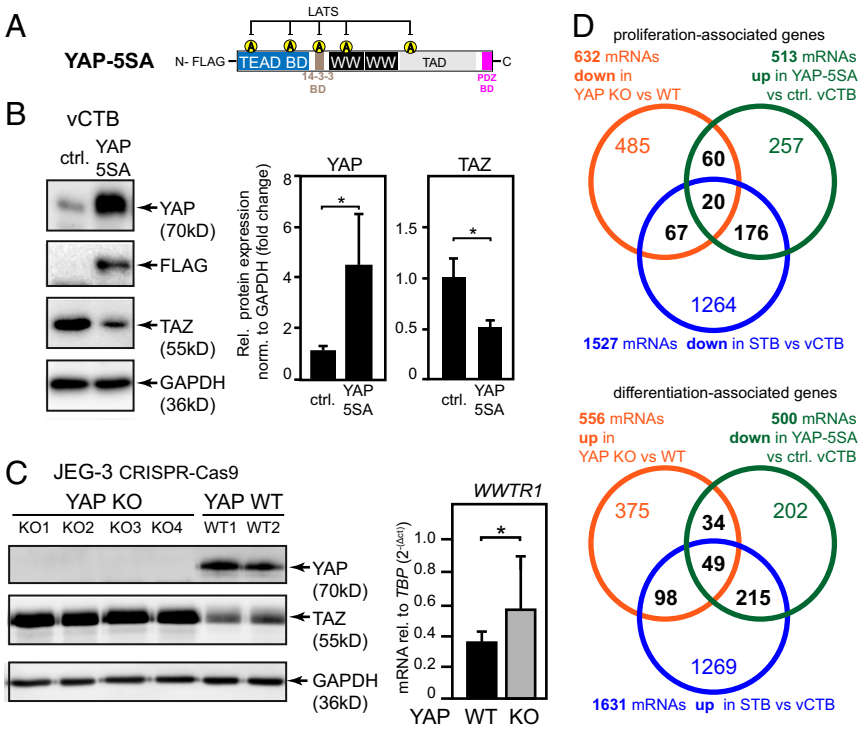

Fig. 2. Genetic YAP manipulation and its genome-wide effects in different trophoblast model systems. (*A*) Schematic presentation of the constitutively active YAP mutant YAP-5SA in which five serine residues (positions 61, 109, 127, 164, and 381) were replaced by alanine. LATS, large tumor suppressor kinase; BD, binding domain; TAD, transactivation domain. (*B*) Representative Western blot and quantification ($n = 3$ preparations isolated from three to five pooled sixth- to eighth-week placentae) demonstrating that YAP-5SA overexpression in primary vCTBs represses TAZ protein levels. GAPDH was used as a loading control. Mean values ± SEM are shown (*Right*; $*P < 0.05$); (*C*) CRISPR-Cas9–mediated YAP gene knock-out in trophoblastic JEG-3 cells elevates TAZ. Representative Western blots of the four established knock-out (KO) and two wildtype (WT) clones are shown. Quantification of *WWTR1* mRNA, encoding TAZ, was performed by qPCR. Mean values ± SEM (normalized to *TBP*) of the four YAP KOs and two WT clones, measured in duplicates, are depicted ($*P < 0.05$). (*D*) Venn diagrams illustrating differentially expressed and commonly regulated genes (based on RNA-seq data) of YAP KO cells (four different KO clones vs. two WT clones), YAP-5SA–overexpressing first-trimester primary vCTBs [$n = 3$ preparations, each isolated from three to five pooled sixth- to eighth-week placentae; YAP-5SA vs. empty (ctrl.) plasmids], and vCTB cultures undergoing STB formation ($n = 3$, isolated from three to five pooled sixth- to seventh-week placentae; 20 h, indicated as vCTB, vs. 72 h, indicated as STB, of cultivation).

human placenta, since they show differential expression in the diverse trophoblast populations and interact with distinct sets of transcription factors. Whereas both YAP and TAZ are absent from hormone-producing STBs, they show an inverse expression pattern in the other trophoblast subtypes. TAZ was found to be weakly expressed in vCTBs and CCTs of early placental tissues, while abundant protein levels were observed in EVTs. In contrast, YAP was strongly expressed in vCTBs and CCTs; however, low amounts were detected in EVTs. Moreover, YAP-5SA overexpression in primary vCTBs decreased, whereas YAP KO in JEG-3 cells increased TAZ protein levels, suggesting a regulatory role of YAP in TAZ expression. Indeed, YAP might impair TAZ stability by promoting its proteasomal degradation, as previously shown in other cells (32). As this study shows that YAP expression is primarily associated with trophoblast stemness and proliferation, YAP-mediated suppression of TAZ could represent a mechanism limiting EVT differentiation, thereby ensuring rapid expansion of the placenta during early pregnancy. The precise role of TAZ in EVTs, however, awaits further investigations. At present, we speculate that it could regulate trophoblast migration, as shown for other epithelial cells, and/or promote epithelial to mesenchymal transition, which occurs during physiological EVT differentiation and can be triggered by aberrant TAZ activation provoking tumorigenesis and metastasis (45–47). TEAD1 and TEAD2 could be the prime interaction partners of TAZ due to their abundance in EVTs. On the contrary, TAZ was also shown to be required for TGF-β signaling by promoting nuclear retention of canonically activated SMAD2/3 (48). Since, in first-trimester placentae, p-SMAD2/3 predominantly localize to nuclei of EVTs (49), TAZ might also play a particular role in the TGF-β responsiveness of migratory trophoblasts.

In contrast to that, YAP has its main function in vCTBs promoting their growth and expansion. Due to the abundance of TEAD4 and its interaction with YAP in vCTBs, nuclear YAP–TEAD4 complexes could be the main drivers of trophoblast proliferation and survival

Besides TEAD4, TEAD3 also bound to YAP in vCTBs and could contribute to trophoblast growth. However, based on its placental expression pattern, TEAD3 might exert its main role in STBs where YAP is absent. Instead, vestigial-like (VGLL) proteins 3 and 4 might act as cofactors (50). Whereas VGLL1 is specifically expressed in vCTBs (27), differentiating trophoblasts express *VGLL4* and *VGLL3*, the latter increasing during 2D cell fusion (29).

Like in other cell types with proliferative and/or stem/progenitor cell-like features (19, 21, 22), YAP seems to trigger vCTB expansion by regulating numerous genes. Overexpression of constitutive active YAP-5SA increased EdU labeling as well as mRNA and protein expression of canonical Hippo targets promoting stemness (CYR61, TEAD4), cell cycle progression (CDK6, CCNA), and survival (PAGE4). Indeed, ChIP-qPCR unraveled direct binding of both YAP and TEAD4 to enhancer/promoter elements of *CCNA2* and *CDK6*. Moreover, inspection of differentially expressed gene lists (Dataset S1) revealed YAP-5SA–dependent up-regulation of other previously identified, direct YAP/TAZ target genes (25), such as

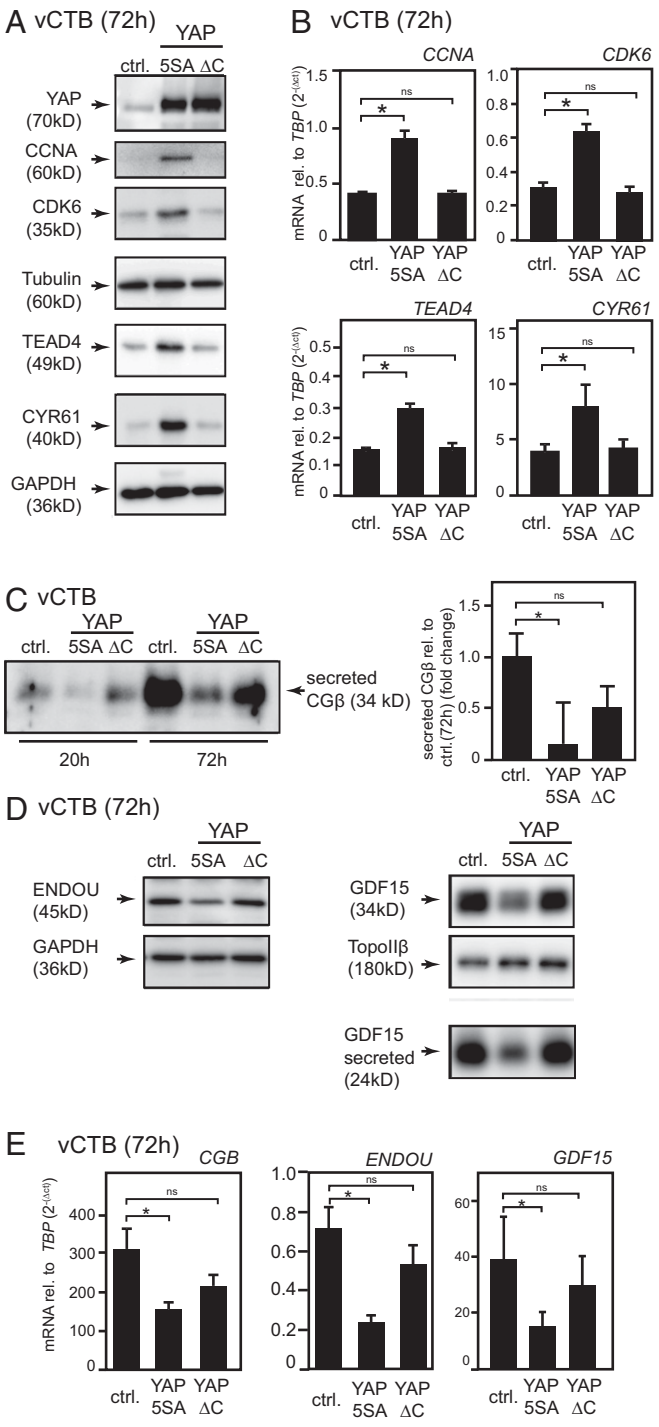

Fig. 3. YAP up-regulates cell cycle genes and suppresses STB markers. Detection of proteins (*A*) and mRNAs (*B*) associated with stemness and proliferation in villous cytotrophoblast (vCTB; $n = 3$ preparations, each isolated from three to five pooled sixth- to eighth-week placentae) after overexpression of YAP-5SA, YAP-ΔC, or empty plasmids (ctrl). GAPDH and tubulin (*A*) were used as loading controls. Transcript levels (*B*) were normalized to *TBP*. (*C*) Representative Western blot ($n = 4$ isolations from three to five pooled sixth- to eighth-week placentae) and quantification (at 72 h) of CGβ protein levels secreted from differentiating vCTBs expressing YAP-5SA, YAP-ΔC, or empty plasmids. (*D*) Immunodetection of ENDOU and GDF15 after transfection with the three different plasmids in vCTBs (representative blots at 72 h are shown). (*E*) qPCR quantification (duplicates) of *CGB*, *ENDOU*, and *GDF15* mRNAs in lysates of transfected vCTBs ($n = 4$ per condition) undergoing STB formation (72 h). All bar graphs depict mean values ± SEM (*$P < 0.05$); ns, not significant.

proliferation/cell cycle-associated transcription factors (*MYBL1*, *ETS1*) and receptors (*AXL*), cytokinesis genes (*KIF20B*, *KIF23*), DNA replication (*TOP2A*) and mitosis-associated factors (*AURKA, PLK1, BUB1, CDK1, CDCA8*), as well as 11 genes encoding different centromere proteins (*CENP*s). Moreover, mRNAs associated with stemness in other cell types such as *HSPD1*, *SKP2*, and *NAP1L1* were significantly increased in the RNA-seq data of YAP-5SA–overexpressing vCTBs. In agreement with that, many of these genes were significantly down-regulated at the protein and/or mRNA level in YAP KO cells (for example, *CYR61*, *TEAD4*, *CDK6*, and several centromere genes; Dataset S2) or showed a trend toward lowered transcript levels in the RNA-seq data. Besides these canonical YAP-TEAD targets, YAP-5SA/YAP KO also indirectly affected genes controlling cell cycle, self-renewal, or survival (Dataset S4). The latter was demonstrated by lower levels of the apoptotic KRT18 neoepitope in YAP-5SA–expressing vCTBs and its up-regulation in trophoblastic JEG-3 cells upon combined YAP/TAZ gene silencing. Indeed, several prosurvival genes, for example, *BIRC5*, commonly known as survivin, and *BAG2*, were elevated, whereas apoptosis-associated genes (*BMF*, *XAF1*, *PML*) were diminished in YAP-5SA–expressing vCTBs (Dataset S1). However, chemical inhibition of both YAP/TAZ in TB-ORGs or YAP KO in JEG-3 organoids primarily affected proliferation of the CTB layer and not its survival. Hence, the mechanical properties of the culture system, such as stiffness of the surrounding 3D matrix (25, 51), likely determine the specific biological effects of Hippo signaling on trophoblasts.

Besides general regulators of proliferation, YAP-5SA also increased markers of vCTB identity such as *CDX2*, *THBS1*, and *ITGA6*, whereas *ITGA1* and *ITGA5*, predominantly expressed by EVTs (52), were down-regulated (Dataset S1). Therefore, YAP may not only trigger trophoblast proliferation by promoting expression of cell cycle and stemness genes, but also by inhibiting differentiation. In particular, down-regulation of STB-specific genes and regulators of cell fusion could be crucial for YAP-dependent vCTB expansion in early pregnancy. Of 1,631 genes up-regulated during STB formation, 264 were suppressed by constitutively active YAP, encoding numerous STB markers (e.g., *ENDOU*, *PLAC4*, *CSFR1*, *ENG*, *SDC1*) and genes encoding pregnancy hormones (*PGF*, *GDF15*; Dataset S4). In addition, transcriptional regulators *GCM1* and *OVOL1* (53, 54) and genes (*CGA*, *CGB3*, *CGB5*, *CGB7*, *CGB8*) encoding the fusogenic hormone hCG (55) were significantly down-regulated by YAP-5SA. As a possible consequence, STB formation was reduced by YAP-5SA in 2D-differentiating vCTBs, whereas YAP KO in JEG-3 cells or chemical inhibition of YAP/TAZ by verteporfin in TB-ORGs promoted syncytialization.

However, the effects of YAP on STB formation could be indirect. Changes in the expression of STB markers could be largely a consequence of elevated CTB growth in cultures with chemically or genetically manipulated YAP. Yet, bioinformatic analyses revealed that the *CGB* gene cluster harbors TEAD4 binding sites in the vicinity of its different coding sequences. Indeed, ChIP-qPCR showed that TEAD4 and/or YAP binding was enriched in the promoter sequences of the *CGB5* and *CGB7* genes upon YAP-5SA overexpression, associated with the up-regulation of the H3K27me3 methyltransferase EZH2 and the repressive histone mark H3K27me3 (56). Therefore, YAP–TEAD4–EZH2 complexes could be required to silence transcription of a subset of STB-specific genes/regulators and thereby suppress cell fusion.

YAP has been previously shown to be critical for self-renewal and expansion of intestinal stem cells in 3D organoids, triggered by stiff designer matrices (57, 58). Similarly, expanding TSCs in Matrigel-embedded 3D TB-ORGs display nuclear YAP and require active YAP/TAZ signaling for self-renewal. It is noteworthy that nuclear YAP coincides with higher numbers of β-catenin–positive nuclei in proliferative trophoblasts of TB-ORGs compared to the villous epithelium in situ (29). Nuclear recruitment of YAP

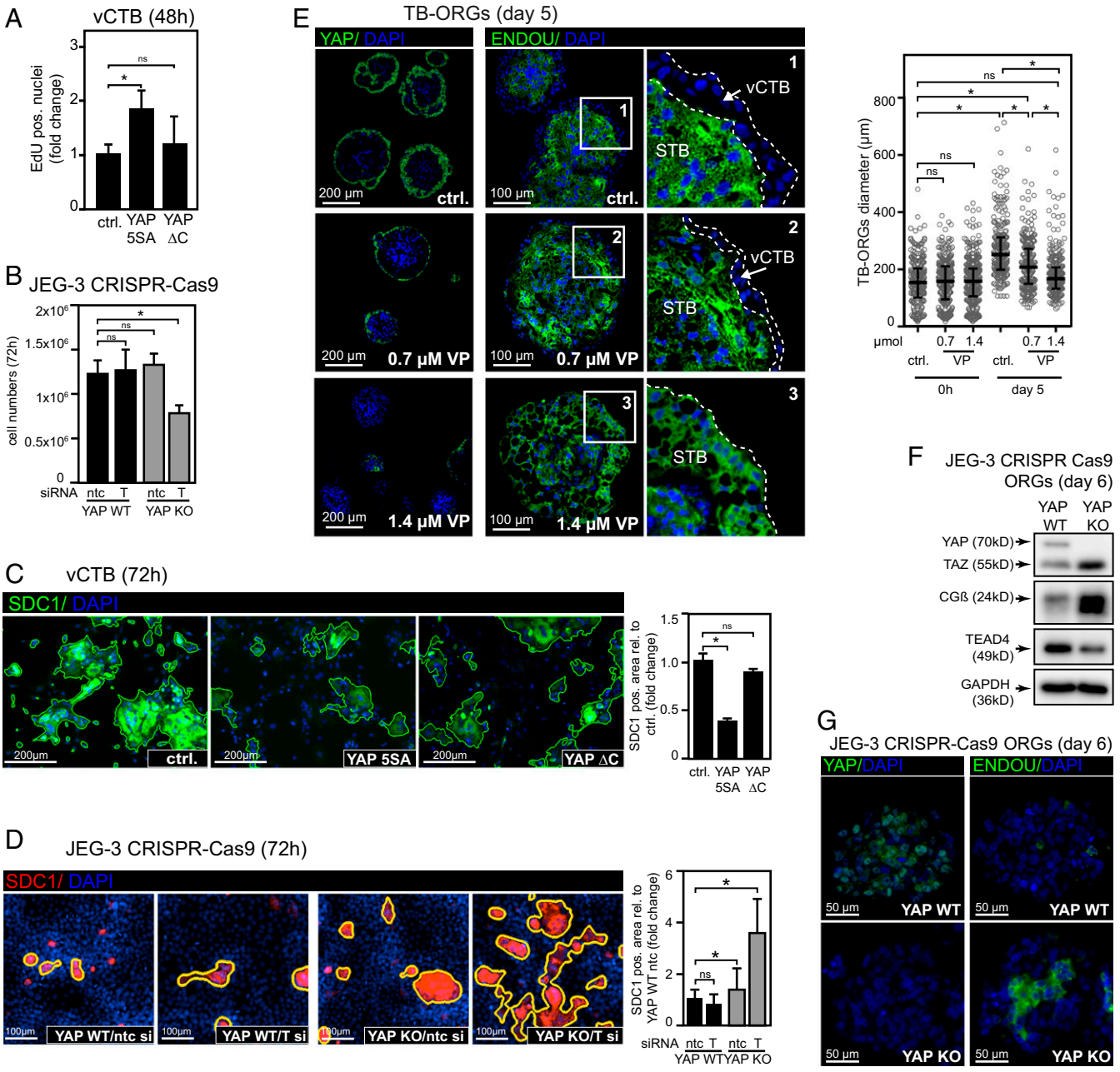

Fig. 4. YAP promotes trophoblast proliferation and inhibits STB formation. (*A*) YAP-5SA overexpression increases EdU labeling of primary vCTBs. Mean values ± SEM ($n = 7$; three to five sixth- to eighth-week placentae per preparation) are shown (*$P < 0.05$); ns, not significant. (*B*) Cell numbers of YAP WT and KO clones 72 h after splitting. Mean values ± SEM ($n = 2$ experiments each using two YAP WT and three YAP KO clones) are depicted. T, TAZ siRNA; ntc, nontargeting control siRNA. (*C*) YAP-5SA impairs syncytialization of primary vCTBs. Representative immunofluorescence images stained with the STB marker syndecan 1 (SDC1) are shown. DAPI marks nuclei. Areas containing SDC1$^+$ STBs, indicated by stippled lines, were quantified 72 h after transfection with YAP-5SA, YAP-ΔC, or empty plasmids. Mean values ± SEM ($n = 3$ vCTB preparations of three to five pooled sixth- to eighth-week placentae) are shown. (*D*) Cell fusion of YAP WT and KO clones treated with TAZ or ntc siRNAs for 72 h. Mean values ± SEM ($n = 3$ with two YAP WT and two YAP KO clones) are shown. (*E*) Self-renewing trophoblast organoids (TB-ORGs) prepared from sixth-week CTBs were treated with two different doses of the YAP/TAZ inhibitor verteporfin (VP) for 5 d. Representative immunostainings for YAP and the STB marker ENDOU are shown. ctrl, untreated control. Stippled lines mark the width of the expanding CTB layer. Graph on the right side depicts organoid size cultivated in the absence (ctrl.) or presence of VP for 5 d. Median values calculated from each 270–395 TB-ORGs (passage 3 to 4) are shown. (*F*) Representative Western blots show diminished TEAD4 and elevated CGβ protein expression in YAP KO organoids (ORGs; $n = 3$). Antibodies simultaneously detecting YAP and TAZ were utilized. GAPDH was used as loading control. (*G*) Representative immunofluorescence pictures of ORGs prepared from YAP WT and KO clones ($n = 2$ experiments) 6 d after ORG formation. DAPI marks nuclei. ORGs generated from YAP KOs show ENDOU-positive areas in the center.

in the Hippo-off state could dissolve the cytoplasmic β-catenin destruction complex, requiring YAP/TAZ for its functionality, and thereby provoke nuclear accumulation of β-catenin (59). The latter may bind to TCF-1, enriched in TB-ORGs (29), and thereby ensure self-renewal of TCSs. In conclusion, we speculate that the cross-talk between canonical Wnt signaling and the Hippo-off state could be crucial for expandability of TSCs in TB-ORGs.

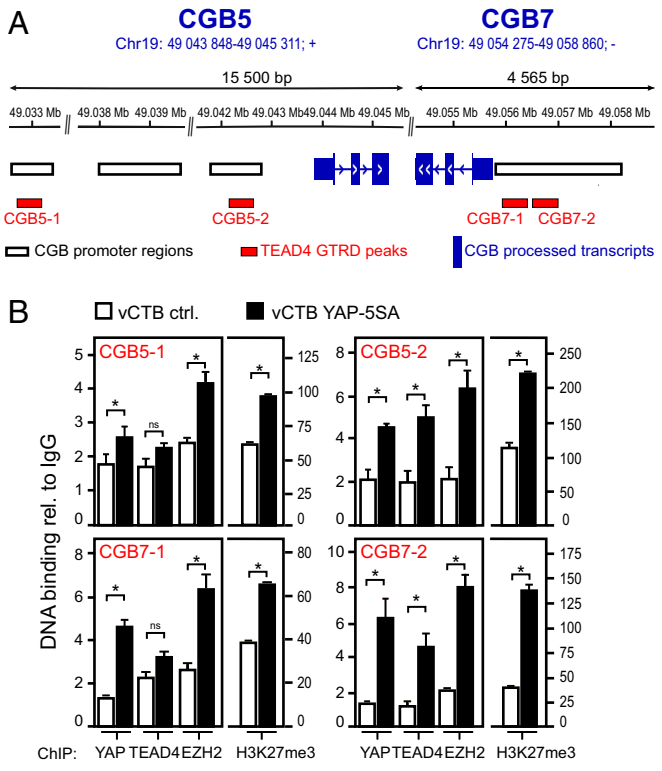

Fig. 5. Repressive YAP–TEAD4–EZH2 complexes bind to TEAD4 cognate sequences of *CGB* genes. (*A*) Schematic representation of *CGB5* and *CGB7* based on data available in the Ensembl genome browser (41). Chromosomal localization of genes, orientation, and promoter regions are depicted. TEAD4 binding regions, previously shown to interact with TEAD4 (depicted in red), were identified by data mining of the GTRD database. (*B*) ChIP-qPCR using two different chromatin pools isolated from purified vCTBs expressing YAP-5SA or empty vectors (ctrl). For each pool, chromatin was combined from three different vCTB preparations (total of 10 to 12 sixth- to eighth-week placentae). Four different qPCR primer sets spanning the predicted TEAD binding sites were chosen. Trimethylation of H3K27 and binding of each YAP, TEAD4, and EZH2 were normalized to ChIP using IgG control. Mean values ± SEM, measured in triplicates, are shown ($P < 0.05$); ns, not significant.

In summary, the coactivator YAP, binding to TEAD4, seems to play a pivotal role in proliferation and expansion of progenitors and TSCs of the villous trophoblast epithelium, supporting the idea that the Hippo signaling pathway could be a main driver of placental development. This finding is in agreement with an accompanying study of Saha et al. showing that TEAD4 is critical for self-renewal of human and postimplantation mouse TSCs. Nuclear YAP–TEAD4 complexes interact with TEAD4 cognate sequences present in the genomic regions of cell cycle regulators and stemness genes and provoke their up-regulation (Fig. 6). Concomitantly, repressive YAP–TEAD4–EZH2 complexes bind to the promoter regions of *CGB* genes, thereby impairing autocrine, hCG-dependent cell fusion and differentiation. Future studies should elucidate the role of other transcriptional regulators potentially controlled by YAP (60) and delineate the cross-talk of Hippo signaling to other developmental cascades such as Wnt and Notch in human trophoblasts.

Materials and Methods

Tissue Collection. Placental tissues (sixth to ninth weeks of gestation) were obtained from legal pregnancy terminations. Utilization of tissues and experimental procedures were approved by the ethical committee of the Medical University of Vienna, requiring written informed consent from women donating their placentae.

Immunofluorescence of Paraffin-Embedded Tissues. Placental tissues and ORGs were fixed in 7.5% formaldehyde and embedded in paraffin. Serial sections (3 μm) of paraffin-embedded material were analyzed by immunofluorescence as described elsewhere (28). Briefly, sections were deparaffinized in Xylol and rehydrated. Antigen retrieval was performed using 1× PT module buffer 1 (Thermo Scientific) for 35 min at 93 °C using a KOS microwave Histostation (Milestone). Slides were incubated with primary antibodies (listed in *SI Appendix*, Table S1) overnight at 4 °C, washed three times, and subsequently incubated with secondary antibodies (2 μg/mL, 1 h; *SI Appendix*, Table S1). Nuclei were stained with 1 μg/mL DAPI. Tissues were analyzed by fluorescence microscopy (Olympus BX50; CellP Software) and digitally photographed.

Immunofluorescence of Cultured Cells. JEG-3 cells and differentiating primary vCTBs were fixed with 4% paraformaldehyde (10 min), treated with blocking buffer (Cell Signaling), and incubated with primary antibodies overnight at 4 °C (listed in *SI Appendix*, Table S1). Next, cells were washed and incubated with 2 μg/mL of secondary antibodies (1 h; *SI Appendix*, Table S1). Nuclei were stained with DAPI. Slides were analyzed by fluorescence microscopy using Lionheart FX equipped with Gen5 software.

Isolation and Cultivation of First-Trimester vCTBs and EVTs. Primary cells were isolated by consecutive enzymatic digestion of pooled sixth- to eighth-week placentae ($n = 3$ to 5 per isolation) as described elsewhere (29). Briefly, digestion 1 was utilized for immune purification of HLA-G$^+$ EVTs as recently described (28). The second and third digestion solutions, mainly containing vCTBs, were pooled and further purified using Percoll density gradient centrifugation (10–70% [vol/vol]; GE Healthcare). Cells were collected between 35 and 50% of Percoll layers, and contaminating red blood cells were removed with erythrocyte lysis buffer for 5 min at room temperature (RT) as described (29). Afterward, cells were seeded onto fibronectin-coated culture dishes at a density of 3×10^5 cells/cm^2 for 20 and 72 h. Supernatants were collected, and differentiating vCTBs were either fixed for immunofluorescence analyses or snap-frozen for qPCR, RNA-seq, and Western blotting. For preparation of cytoplasmic and nuclear extracts, NE-PER extraction reagent was used according to the manufacturer's instructions (Pierce). For quantification of cell fusion, vCTB cultures were stained with syndecan-1 (SDC-1)/DAPI and photographed. The ratio of SDC-1–positive areas to DAPI was measured using Gen5 software (Lionheart FX).

TB-ORGs and JEG-3 ORGs. TB-ORGs and JEG-ORGs were generated by embedding primary vCTBs (sixth to seventh week) and JEG-3 cells (YAP WT or knock-out clones), respectively, in 60% growth factor-reduced Matrigel. ORGs were cultivated in basic trophoblast organoid medium containing 1 mM A83-01 (R&D Systems), 100 ng/mL recombinant human epidermal growth factor (rhEGF; R&D Systems), and 3 mM CHIR99021 (Tocris) as previously mentioned (29). For chemical inhibition of YAP/TAZ, TB-ORGs

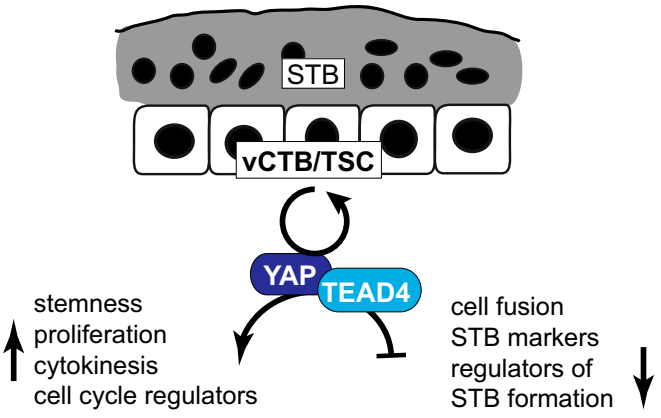

Fig. 6. Picture illustrating the role of YAP–TEAD4 complexes in the villous trophoblast epithelium. YAP–TEAD4 complexes bind to stemness and cell cycles genes, increase their expression, and thereby promote vCTB/TSC expansion. Concurrently, YAP–TEAD4 complexes also inhibit cell fusion and STB marker expression by forming gene-repressive complexes in their promoter regions.

were split and verteporfin (Sigma) was added at concentrations of 0.7 and 1.4 μM for 5 d. ORGs were photographed, and diameter of individual ORGs was measured by using Adobe Photoshop CS5.

Transfection of Primary vCTBs. Isolated vCTBs were transfected (4D-Nucleofector program EO-100; Lonza) with plasmids encoding pCMV-flag YAP2-5SA [Addgene plasmid no. 27371 (32)], p2×Flag CMV2-YAP2-ΔC [Addgene plasmid no. 21123 (34)], or pcDNA3.1(−) (control plasmid) using the AMAXA SG Cell line kit. Transfection with a pmaxGFP (Lonza) revealed an average transfection efficiency of 20 to 30%. Next, vCTBs were seeded onto fibronectin and incubated up to 120 h at 37 °C.

YAP Gene Knock-Out. JEG-3 cells (30 to 40% confluency) were transfected with 0.5 μg of two different plasmids encoding YAP sgRNA and Cas9 (HCP000693-CG01-2-B-a and HCP000693-CG01-2-B-b; two different sgRNAs; GeneCopoeia) and a donor vector (donor with YAP GFP replacement; DC-HTN000693-DO1; 1 μg) using DNAfectin Plus (ABM). For generation of JEG-3 wild type clones, cells were transfected with plasmids encoding a non-targeting control sgRNA (CCPTR01-1-CG01; GeneCopoeia). After cultivation for 24 h in DMEM (Gibco) containing 10% FBS (Biochrom) and 2 mM L-glutamine (Gibco), cells were split and treated with G418 (800 μg/mL for 24 h) and 1 μg/mL puromycin. After ∼2 wk, single clones were picked, transferred to 96-well plates, and analyzed by qPCR, Western blotting, and immunofluorescence using YAP antibodies. For long-term cultivation, clones were maintained in the presence of 0.5 μg/mL puromycin.

Gene Silencing in vCTBs and JEG-3 Cells. For siRNA-mediated gene silencing, a mixture of four different siRNAs targeting YAP (L-012200-00-0005) or TAZ (L-016083-00-0005; ON-TARGETplus SMARTpools; Dharmacon) or a non-targeting (si-ctrl) control pool (D-001810-10-20) was transfected by using Lipofectamine RNAiMAX as described (61).

Quantitative PCR (qPCR). After RNA isolation (PeqGold Trifast; PeqLab) and reverse transcription (RevertAid H Minus Reverse Transcriptase; Thermo Scientific), qPCR was performed using a 7500 Fast Real-time PCR system (Applied Biosystems) as described (28). The following TaqMan Gene Expression Assays (ABI) were utilized: TEAD1 (Hs00173359_m1), TEAD2 (Hs00366217_m1), TEAD3 (Hs00243231_m1), TEAD4 (Hs01125032_m1), CDX2 (Hs01078080_m1), CCNA2 (Hs00996788_m1), CDK6 (Hs01026371_m1), CYR61 (Hs00998500_g1), CGB (Hs00361224_gH), ENDOU (Hs00195731_m1), GDF15 (Hs00171132_m1), PAGE4 (Hs00199655_m1), ITGA6 (Hs01041011_m1), GCM1 (Hs00961601_m1), OVOL1 (Hs00190060_m1), p63 (Hs00978340_m1), YAP (Hs00902712_g1), and WWTR1 (Hs00210007_m1). Signals (ΔCt) were normalized to TATA-box binding protein (TBP, 4333769F).

Western Blotting. Protein extracts and culture supernatants were separated on SDS/PAA gels, transferred onto Hybond-P PVDF (GE Healthcare) membranes, and incubated overnight with primary antibodies (*SI Appendix*, Table S1) at 4 °C as described previously (28). Subsequently, filters were washed and incubated for 1 h with HRP-conjugated secondary antibodies (*SI Appendix*, Table S1). Signals were developed using WesternBright Chemiluminescenz Substrat Quantum (Biozym) and visualized with a ChemiDoc Imaging System (Bio-Rad). Quantification was performed by using ImageJ software.

Immunoprecipitation. Cells (2×10^6 HLA-G$^+$ EVTs and vCTBs) were isolated as described earlier. Preparation of protein lysates and immunoprecipitation using YAP antibodies or rabbit IgG controls (listed in *SI Appendix*, Table S1) was performed according to manufacturer's instructions (Cell Signaling, no. 73778). Coimmunoprecipitating proteins (TEAD1, 3, 4) were detected by Western blotting.

Luciferase Reporter Assay. Cells were cotransfected with 2 μg/mL of a luciferase reporter [8× GTII-luciferase; Addgene plasmid no. 34615 (62)] containing eight TEAD binding sites (ACATTCCA) and 0.5 μg/mL pCMV–β-galactosidase (CMV-βGal; normalization control) using DNAfectin Plus. Luciferase activity and β-galactosidase activity were determined as previously published (43).

Proliferation Assays. Purified vCTBs were transfected with YAP-5SA, YAP2-ΔC, or control plasmids [pcDNA3.1(-)] seeded onto fibronectin-coated dishes and incubated for 24 h. Afterward, 10 μM 5-ethynyl-2′-deoxyuridine (EdU; EdU-Click 488, BaseClick) was added for 24 h. Subsequently, cells were fixed and EdU was detected according to the manufacturer's instructions. Nuclei were stained with DAPI. Cells were digitally photographed (10 pictures per condition) using Lionheart FX, and EdU-positive nuclei were counted using Gen5 software. JEG-3 cell proliferation was quantified by measuring cumulative cell numbers after 24, 48, and 72 h of cultivation using a Casy cell counting system (Schärf System).

Chromatin Immunoprecipitation (ChIP)-qPCR. For ChIP analyses, SimpleChIP Enzymatic Chromatin IP Kit (Cell Signaling) was used as described by the manufacturer. Briefly, vCTBs were transfected with YAP-5SA and control plasmids, seeded onto fibronectin-coated dishes, and incubated for 20 h. Next, cells were fixed with 1% formaldehyde (10 min). After nuclei preparation, chromatin digestion, and sonication, purified chromatin lysates were incubated either with YAP, TEAD4, EZH2, H3K27me3 (*SI Appendix*, Table S1), or normal rabbit IgG (negative control) overnight at 4 °C. Immunoprecipitated chromatin was captured with ChIP-Grade Protein G Magnetic Beads and eluted. Purified DNA was assessed by qPCR (7500 Fast Real-time PCR system) using ABI BrightGreen Express 2× qPCR MasterMix (ABM) according to the manufacturer's instruction. Primers amplifying genomic regions with TEAD4 binding sites are indicated in *SI Appendix*, Table S2. Relative occupancy of YAP, TEAD4, EZH2, and H3K27me3 was normalized to normal rabbit IgG.

RNA-Seq. For RNA-seq, total RNA was prepared by using an AllPrep DNA/RNA/miRNA Universal Kit. Sequencing libraries were be prepared at the Core Facility Genomics, Medical University of Vienna, using the NEBNext Poly(A) mRNA Magnetic Isolation Module and the NEBNext Ultra II Directional RNA Library Prep Kit for Illumina according to manufacturer's protocols (New England Biolabs). Libraries were QC-checked on a Bioanalyzer 2100 (Agilent) using a High Sensitivity DNA Kit for correct insert size and quantified using Qubit dsDNA HS Assay (Invitrogen). Pooled libraries were sequenced on a NextSeq500 instrument (Illumina) in 1 × 75-bp single-end sequencing mode.

RNA-Seq Data and Analysis. FASTQ files were generated by Illumina's pipeline, and read quality was assessed by FastQC (http://www.bioinformatics.babraham.ac.uk/projects/fastqc/). Subsequently, reads were submitted to alignment with HISAT2 (v2.1.0; PMID 25751142). The mapping was made using default parameters with reference human genome GRCh38. Aligned BAM files were indexed and sorted with Samtools (v0.1.18; PMID 19505943) for downstream analysis. Genomic features and read count matrices were obtained using featureCounts (v1.5.2; PMID 24227677) based on annotation file hg38 (RefSeq track of UCSC Table Browser). Differential gene expression analysis was performed using the R package DESeq2 (PMID 20979621, 25516281). Criteria for differentially expressed genes were: values >100; fold change >1.5, false discovery rate <0.2. Venn diagrams were built by using BioVenn as described (63). Heat maps were constructed by using Clustvis (64).

Identifying TEAD4 Binding Sites in the Regulatory Regions of Genes. TEAD4 binding regions from published ChIP-seq experiments were retrieved from the GTRD database as nonredundant metaclusters (PMID 30445619). The regulatory regions were searched for TEAD4 binding motifs using the FIMO program (PMID 21330290) with the M06183_1.94d position weight matrix retrieved from the Human TFs website (PMID 29425488), with the *P* value threshold set to 0.0001.

Statistical Analyses. Gaussian distribution was examined using D'Agostino–Pearson normality test, and equality of variances was examined with Bartlett's test using GraphPad Prism 6.01. Statistical analysis of data between two means was performed with Student's *t* test or Mann–Whitney *U* test. Comparisons of multiple groups were evaluated with one-way ANOVA and appropriate post hoc tests or Kruskal–Wallis tests. A *P* value of <0.05 was considered statistically significant.

Data Availability Statement. Raw RNA-seq data are accessible at the Gene Expression Omnibus (GEO) database (accession nos. GSE143858, GSE143859, and GSE143860).

ACKNOWLEDGMENTS. This study was supported by the Austrian Science Fund (Grants P-28417-B30 and P31470-B30), the Hungarian Academy of Sciences (Grant LP2014-7/2014), the Hungarian Scientific Research Fund (Grants OTKA K124862 and K128262), and the Hungarian National Research, Development and Innovation Fund (Grant FIEK_16-1-2016-0005).

1. G. J. Burton, A. L. Fowden, The placenta: A multifaceted, transient organ. *Philos. Trans. R. Soc. Lond B Biol. Sci.* **370**, 20140066 (2015).
2. A. Erlebacher, Immunology of the maternal-fetal interface. *Annu. Rev. Immunol.* **31**, 387–411 (2013).
3. T. Napso, H. E. J. Yong, J. Lopez-Tello, A. N. Sferruzzi-Perri, The role of placental hormones in mediating maternal adaptations to support pregnancy and lactation. *Front. Physiol.* **9**, 1091 (2018).
4. R. Pijnenborg, L. Vercruysse, M. Hanssens, The uterine spiral arteries in human pregnancy: Facts and controversies. *Placenta* **27**, 939–958 (2006).
5. J. Hustin, E. Jauniaux, J. P. Schaaps, Histological study of the materno-embryonic interface in spontaneous abortion. *Placenta* **11**, 477–486 (1990).
6. T. Y. Khong, F. De Wolf, W. B. Robertson, I. Brosens, Inadequate maternal vascular response to placentation in pregnancies complicated by pre-eclampsia and by small-for-gestational age infants. *Br. J. Obstet. Gynaecol.* **93**, 1049–1059 (1986).
7. R. Pijnenborg *et al*., Placental bed spiral arteries in the hypertensive disorders of pregnancy. *Br. J. Obstet. Gynaecol.* **98**, 648–655 (1991).
8. R. Romero, J. P. Kusanovic, T. Chaiworapongsa, S. S. Hassan, Placental bed disorders in preterm labor, preterm PROM, spontaneous abortion and abruptio placentae. *Best Pract. Res. Clin. Obstet. Gynaecol.* **25**, 313–327 (2011).
9. W. T. Parks, Placental hypoxia: The lesions of maternal malperfusion. *Semin. Perinatol.* **39**, 9–19 (2015).
10. E. Weiner *et al*., Placental histopathological lesions in correlation with neonatal outcome in preeclampsia with and without severe features. *Pregnancy Hypertens.* **12**, 6–10 (2018).
11. G. J. Burton, E. Jauniaux, Placental oxidative stress: From miscarriage to preeclampsia. *J. Soc. Gynecol. Investig.* **11**, 342–352 (2004).
12. N. G. Than *et al*., Integrated systems Biology approach identifies novel maternal and placental pathways of preeclampsia. *Front. Immunol.* **9**, 1661 (2018).
13. K. H. Lim *et al*., Human cytotrophoblast differentiation/invasion is abnormal in pre-eclampsia. *Am. J. Pathol.* **151**, 1809–1818 (1997).
14. C. P. Chen, R. Bajoria, J. D. Aplin, Decreased vascularization and cell proliferation in placentas of intrauterine growth-restricted fetuses with abnormal umbilical artery flow velocity waveforms. *Am. J. Obstet. Gynecol.* **187**, 764–769 (2002).
15. M. A. Costa, Scrutinising the regulators of syncytialization and their expression in pregnancy-related conditions. *Mol. Cell. Endocrinol.* **420**, 180–193 (2016).
16. C. P. Chen *et al*., Altered placental syncytin and its receptor ASCT2 expression in placental development and pre-eclampsia. *BJOG* **113**, 152–158 (2006).
17. I. Knerr, E. Beinder, W. Rascher, Syncytin, a novel human endogenous retroviral gene in human placenta: Evidence for its dysregulation in preeclampsia and HELLP syndrome. *Am. J. Obstet. Gynecol.* **186**, 210–213 (2002).
18. R. M. Sheridan, J. Stanek, J. Khoury, S. Handwerger, Abnormal expression of transcription factor activator protein-2α in pathologic placentas. *Hum. Pathol.* **43**, 1866–1874 (2012).
19. X. Varelas, The Hippo pathway effectors TAZ and YAP in development, homeostasis and disease. *Development* **141**, 1614–1626 (2014).
20. F. X. Yu, K. L. Guan, The Hippo pathway: Regulators and regulations. *Genes Dev.* **27**, 355–371 (2013).
21. B. Zhao, K. Tumaneng, K. L. Guan, The Hippo pathway in organ size control, tissue regeneration and stem cell self-renewal. *Nat. Cell Biol.* **13**, 877–883 (2011).
22. I. M. Moya, G. Halder, Hippo-YAP/TAZ signalling in organ regeneration and regenerative medicine. *Nat. Rev. Mol. Cell Biol.* **20**, 211–226 (2019).
23. J. R. Misra, K. D. Irvine, The Hippo signaling network and its biological functions. *Annu. Rev. Genet.* **52**, 65–87 (2018).
24. K. C. Lin, H. W. Park, K. L. Guan, Regulation of the Hippo pathway transcription factor TEAD. *Trends Biochem. Sci.* **42**, 862–872 (2017).
25. A. Totaro, T. Panciera, S. Piccolo, YAP/TAZ upstream signals and downstream responses. *Nat. Cell Biol.* **20**, 888–899 (2018).
26. N. Nishioka *et al*., The Hippo signaling pathway components Lats and Yap pattern Tead4 activity to distinguish mouse trophectoderm from inner cell mass. *Dev. Cell* **16**, 398–410 (2009).
27. F. Soncin *et al*., Comparative analysis of mouse and human placentae across gestation reveals species-specific regulators of placental development. *Development* **145**, dev156273 (2018).
28. S. Haider *et al*., Notch1 controls development of the extravillous trophoblast lineage in the human placenta. *Proc. Natl. Acad. Sci. U.S.A.* **113**, E7710–E7719 (2016).
29. S. Haider *et al*., Self-renewing trophoblast organoids recapitulate the developmental program of the early human placenta. *Stem Cell Reports* **11**, 537–551 (2018).
30. H. Okae *et al*., Derivation of human trophoblast stem cells. *Cell Stem Cell* **22**, 50–63.e6 (2018).
31. B. Huppertz, M. Gauster, Trophoblast fusion. *Adv. Exp. Med. Biol.* **713**, 81–95 (2011).
32. B. Zhao *et al*., Inactivation of YAP oncoprotein by the Hippo pathway is involved in cell contact inhibition and tissue growth control. *Genes Dev.* **21**, 2747–2761 (2007).
33. M. L. Finch-Edmondson *et al*., TAZ protein accumulation is negatively regulated by YAP abundance in mammalian cells. *J. Biol. Chem.* **290**, 27928–27938 (2015).
34. T. Oka, M. Sudol, Nuclear localization and pro-apoptotic signaling of YAP2 require intact PDZ-binding motif. *Genes Cells* **14**, 607–615 (2009).
35. G. Meinhardt, M. Knöfler, S. Hetey, A. Szilagyi, Next Generation Sequencing of first trimester human cytotrophoblasts expressing a constitutively active mutant (5SA) of the transcriptional co-activator YAP. Gene Expression Omnibus. https://www.ncbi.nlm.nih.gov/geo/query/acc.cgi?acc=GSE143858. Deposited 17 January 2020.
36. G. Meinhardt, M. Knöfler, S. Hetey, A. Szilagyi, Comparison of CRISPR-Cas9 genome-edited JEG-3 YAP knockout and wild type choriocarcinoma cells. Gene Expression Omnibus. ttps://www.ncbi.nlm.nih.gov/geo/query/acc.cgi?acc=GSE143859. Deposited 17 January 2020.
37. G. Meinhardt, M. Knöfler, S. Hetey, A. Szilagyi, Next Generation Sequencing of syncytializing first trimester human cytotrophoblasts. Gene Expression Omnibus. https://www.ncbi.nlm.nih.gov/geo/query/acc.cgi?acc=GSE143860. Deposited 17 January 2020.
38. M. Knöfler *et al*., Human placenta and trophoblast development: Key molecular mechanisms and model systems. *Cell. Mol. Life Sci.* **76**, 3479–3496 (2019).
39. Q. Xie *et al*., YAP/TEAD-mediated transcription controls cellular senescence. *Cancer Res.* **73**, 3615–3624 (2013).
40. F. Zanconato *et al*., Genome-wide association between YAP/TAZ/TEAD and AP-1 at enhancers drives oncogenic growth. *Nat. Cell Biol.* **17**, 1218–1227 (2015).
41. D. R. Zerbino *et al*., Ensembl 2018. *Nucleic Acids Res.* **46**, D754–D761 (2018).
42. M. Y. Turco *et al*., Trophoblast organoids as a model for maternal-fetal interactions during human placentation. *Nature* **564**, 263–267 (2018).
43. G. Meinhardt *et al*., Wnt-dependent T-cell factor-4 controls human etravillous trophoblast motility. *Endocrinology* **155**, 1908–1920 (2014).
44. J. Pollheimer *et al*., Activation of the canonical wingless/T-cell factor signaling pathway promotes invasive differentiation of human trophoblast. *Am. J. Pathol.* **168**, 1134–1147 (2006).
45. S. DaSilva-Arnold, J. L. James, A. Al-Khan, S. Zamudio, N. P. Illsley, Differentiation of first trimester cytotrophoblast to extravillous trophoblast involves an epithelial-mesenchymal transition. *Placenta* **36**, 1412–1418 (2015).
46. J. H. Park, J. E. Shin, H. W. Park, The role of Hippo pathway in cancer stem cell Biology. *Mol. Cells* **41**, 83–92 (2018).
47. J. E Davies *et al*., Epithelial-mesenchymal transition during extravillous trophoblast differentiation. *Cell Adhes. Migr.* **10**, 310–321 (2016).
48. X. Varelas *et al*., TAZ controls Smad nucleocytoplasmic shuttling and regulates human embryonic stem-cell self-renewal. *Nat. Cell Biol.* **10**, 837–848 (2008).
49. S. Haider, V. Kunihs, C. Fiala, J. Pollheimer, M. Knöfler, Expression pattern and phosphorylation status of Smad2/3 in different subtypes of human first trimester trophoblast. *Placenta* **57**, 17–25 (2017).
50. A. V. Pobbati, W. Hong, Emerging roles of TEAD transcription factors and its co-activators in cancers. *Cancer Biol. Ther.* **14**, 390–398 (2013).
51. G. Brusatin, T. Panciera, A. Gandin, A. Citron, S. Piccolo, Biomaterials and engineered microenvironments to control YAP/TAZ-dependent cell behaviour. *Nat. Mater.* **17**, 1063–1075 (2018).
52. C. H. Damsky, M. L. Fitzgerald, S. J. Fisher, Distribution patterns of extracellular matrix components and adhesion receptors are intricately modulated during first trimester cytotrophoblast differentiation along the invasive pathway, in vivo. *J. Clin. Invest.* **89**, 210–222 (1992).
53. S. J. Renaud *et al*., OVO-like 1 regulates progenitor cell fate in human trophoblast development. *Proc. Natl. Acad. Sci. U.S.A.* **112**, E6175–E6184 (2015).
54. D. Baczyk *et al*., Glial cell missing-1 transcription factor is required for the differentiation of the human trophoblast. *Cell Death Differ.* **16**, 719–727 (2009).
55. M. Yang, Z. M. Lei, C. Rao, The central role of human chorionic gonadotropin in the formation of human placental syncytium. *Endocrinology* **144**, 1108–1120 (2003).
56. Y. H. Chen, M. C. Hung, L. Y. Li, EZH2: A pivotal regulator in controlling cell differentiation. *Am. J. Transl. Res.* **4**, 364–375 (2012).
57. N. Gjorevski *et al*., Designer matrices for intestinal stem cell and organoid culture. *Nature* **539**, 560–564 (2016).
58. M. Imajo, M. Ebisuya, E. Nishida, Dual role of YAP and TAZ in renewal of the intestinal epithelium. *Nat. Cell Biol.* **17**, 7–19 (2015).
59. L. Azzolin *et al*., YAP/TAZ incorporation in the β-catenin destruction complex orchestrates the Wnt response. *Cell* **158**, 157–170 (2014).
60. C. Zhu, L. Li, B. Zhao, The regulation and function of YAP transcription co-activator. *Acta Biochim. Biophys. Sin. (Shanghai)* **47**, 16–28 (2015).
61. M. Rosner *et al*., Efficient siRNA-mediated prolonged gene silencing in human amniotic fluid stem cells. *Nat. Protoc.* **5**, 1081–1095 (2010).
62. S. Dupont *et al*., Role of YAP/TAZ in mechanotransduction. *Nature* **474**, 179–183 (2011).
63. T. Hulsen, J. de Vlieg, W. Alkema, BioVenn - a web application for the comparison and visualization of biological lists using area-proportional Venn diagrams. *BMC Genomics* **9**, 488 (2008).
64. T. Metsalu, J. Vilo, ClustVis: A web tool for visualizing clustering of multivariate data using principal component analysis and heatmap. *Nucleic Acids Res.* **43**, W566–W570 (2015).